Empirical three-body potential for vitreous silica[a)]

B. P. Feuston[b)] and S. H. Garofalini
Department of Ceramics, Rutgers University, Piscataway, New Jersey 08854

(Received 20 May 1988; accepted 27 July 1988)

A three-body potential suitable for molecular dynamics (MD) simulations has been developed for vitreous silica by adding three-body interactions to the Born–Mayer–Huggins (BMH) pair potential. Previous MD simulations with the BMH potential have formed glassy SiO_2 through the melt-quench method with some success. Though bond lengths were found to be in fair agreement with experiment, the distribution of tetrahedral angles was too broad and the model glass contained 6%–8% bond defects. This is indicative of a lack of the local order that is present in the laboratory glass. The nature of the short range order is expected to play an important role when investigating defect formation, surface reconstruction, or surface reactivities. An attempt has been made to increase the local order in the simulated glass by including a directional dependent term in the effective potential to model the partial covalency of the Si–O bond. The vitreous state obtained through MD simulation with this modified BMH potential shows an increase in the short range order with a narrow O–Si–O angle distribution peaked about the tetrahedral angle and a low concentration of bond defects, typically ~1%–2%. The static structure factor $S(q)$ is calculated and found to be in good agreement with neutron scattering results. Intermediate range order is also discussed in reference to the distribution of ring sizes.

I. INTRODUCTION

Important contributions to our understanding of the microscopic structure and dynamics of vitreous silica (v-SiO_2), whose technological significance has long been appreciated, are recently being made through molecular dynamics (MD) computer simulations.[1–11] While experiments accurately measure the average structure and particle dynamics, MD simulations permit detailed analysis of the atomistic motion and the complex microstructure that give rise to the average properties. The disadvantage of classical MD simulations is their reliance upon an effective interaction potential. The ability of this potential to model the real binding energy and atomic forces, and therefore, make accurate predictions, is determined empirically by comparing simulation generated time averages with experimental results. Due to the complex nature of many-body interactions in a condensed matter system, it is unlikely that a single effective potential will be able to reproduce all the physical properties exhibited by a particular system, e.g., all crystalline, amorphous, liquid, and surface states. Subsequently, the adjustable parameters in an effective potential are determined through quantitative agreement with a small subset of the available experimental data, relating to a specific state of the system. In addition to a quantitive analysis of the atomic-level dynamics and structure for the particular state for which it was constructed, the effective potential often leads to a better understanding of other physical states of the system. Though most effective potentials are parametrized by comparison to measured bulk properties, they will often be successfully employed in the investigations of surface reconstruction and reactivities, epitaxial growth, and microclusters.

In the case of SiO_2, several pair potentials have been constructed to simulate the vitreous state, technologically the most important.[1,3,10] The implementation of these potentials in MD simulations has yielded reasonably accurate descriptions of the vitreous state. The glassy state is achieved in MD simulations by "slowly" cooling the equilibrium liquid until diffusion ceases and the system is arrested in a stable or metastable configuration. The low-temperature system can then be annealed to allow further structural relaxation. The cooling rate in MD simulations (typically $\sim 10^{13}$–10^{14} K/s), orders of magnitude higher than those achieved in the laboratory, is limited by practical considerations of computing power. Glasses constructed through this melt-quench procedure, using ionic pair potentials, typically have a large number of bond defects (~6%–8% odd-coordinated Si and O), attributed to the extremely high cooling rates. Nonetheless, MD simulations of vitreous silica and silicate systems using these ionic potentials have yielded dynamical[4] (phonon density of states) and structural[1,2,7–11] (radial distribution function) results that compare favorably with x-ray[12(a)] diffraction and neutron scattering[13(a)] data. These studies have provided new insights into the bulk and surface microstructure, liquid–glass transition, particle diffusion, and surface–adsorbate interactions.

Yet, a more critical analysis of the MD results for v-SiO_2 show that even though the radial distribution function matches the experimental results fairly well, the distribution of O–Si–O bond angles is too broad and the Si–O–Si bond angle too large. These discrepancies in bond angles indicates a lower degree of short range order (SRO) than is apparent in the laboratory glass. The nature of the SRO is crucial

[a)] Work supported in part by the Army Research Office, Grant No. DAAL03-86-K-0047.
[b)] Postdoctoral Fellow of Rutgers University and John von Neumann Supercomputer Center.

 0021-9606/88/215818-07$02.10

when considering defect formation, surface reconstruction, and surface reactivity. It is not surprising that these isotropic two-body potentials fail to reproduce the high degree of local order found in silica, due to the omission of any directional-dependent terms in the effective potential to reflect the partial covalency of the SiO_2 system.

An attempt to correct this omission is made by adding a small three-body interaction term to a modified ionic pair potential to simulate the directional-dependent bonding in SiO_2. Molecular dynamics simulations of bulk silica utilizing this new potential show a well defined local structure centered about the silicon atoms, lower concentration of bond defects, and better agreement with the experimental radial distribution function than the previously used two-body potentials.

In Sec. II the modified Born–Mayer–Huggins pair potential is described in detail and the functional form of the three-body interaction term is introduced phenomenologically. The technique for determining the adjustable parameters in the potential is discussed in Sec. III. The structure of the simulated glass is described in Sec. IV in terms of the radial distribution function (RDF), static structure factor [$S(q)$], angle distributions, bond defects, and ring statistics. Results are summarized in Sec. V.

II. THE POTENTIAL

The cohesive energy of N-interacting atoms can be described by a potential-energy function of the atomic positions $V(\mathbf{r}_1, \mathbf{r}_2, \mathbf{r}_3,...,\mathbf{r}_N)$. In general, V may be expressed as the sum of one-, two-, three-body potentials, etc., as

$$V(\mathbf{r}_1,\mathbf{r}_2,\mathbf{r}_3,...,\mathbf{r}_N) = \sum_i v_1(\mathbf{r}_i) + \sum_{i<j} v_2(\mathbf{r}_i,\mathbf{r}_j) + \sum_{i<j<k} v_3(\mathbf{r}_i,\mathbf{r}_j,\mathbf{r}_k) + \cdots + v_N(\mathbf{r}_1,\mathbf{r}_2,\mathbf{r}_3,...,\mathbf{r}_N) . \quad (2.1)$$

The one-body potential v_1, representive of an external potential, is taken to be zero in the present case. For the above expansion to be reasonable, the dominant potential-energy contribution will then come from pair interactions v_2, while contributions to the total potential energy from the n-body term will be less than the $(n-1)$-atom term, for $3 \leqslant n \leqslant N$. In the special cases of ionic (alkali halides) and van der Waals (inert gases) systems, two-body potentials alone appear to be sufficient in the potential energy expression, Eq. (2.1), as demonstrated through the close agreement between simulation and experimental results.[14,15] But pair potentials, which neglect v_3 and higher order terms, are inadequate for properly describing systems which exhibit covalent bonding, thereby requiring the inclusion of a directional-dependent term in the effective potential. The empirical potential for v-SiO_2 presented here contains, in addition to pair interactions, three-body interactions for simulating the preferred bonding configurations, thus constraining the local order in the model glass.

In the present study, a modified form of the Born–Mayer–Huggins (BMH) ionic potential,[10,11] which has been successfully employed in previous MD simulations of silica and silicate systems, is used to describe pair interactions. The two-body interaction potential has the following functional form:

$$v_2(\mathbf{r}_i,\mathbf{r}_j) = v_2(r_{ij}) = A_{ij} \exp(-r_{ij}/\rho) + (Z_i Z_j e^2/r_{ij})\operatorname{erfc}(r_{ij}/\beta_{ij}) , \quad (2.2)$$

where r_{ij} is the separation distance, Z_i is the formal ionic charge, and ρ, β_{ij} are adjustable parameters. The coefficient of the short range repulsive term is determined by

$$A_{ij} = (1 + Z_i/n_i + Z_j/n_j) * b * \exp[(\sigma_i + \sigma_j)/\rho] , \quad (2.3)$$

where n_i is the number of valence shell electrons, σ_i the ionic radius, and b a constant. Values for σ_i, b, and ρ have been taken from previous MD simulations using the BMH pair potential.[10,11] The difference between the present approach and previous simulations by other authors[1,2] with this potential is the treatment of the long range Coulomb term [second term in Eq. (2.2)]. Previous simulations of silica and silicate glasses have used Ewald's method, with or without the inverse lattice sum, to evaluate the Coulombic interaction. The abbreviated Ewald sum (without the lattice sum) introduces more error into the approximation for $1/r$, but this is not considered serious for v-SiO_2 which is not a completely ionic system. In addition to abbreviating the Ewald sum, the Ewald's convergence parameter [$1/(\eta L)$, where η is a constant and L the MD box length], is treated as a size-independent, interaction-dependent adjustable parameter $(1/\beta_{ij})$.[10,11] In essence, the strength of the Coulombic interaction between two "ions" of charge Z_i and Z_j assumes a distance dependence,

$$Z_i Z_j \rightarrow Z_i Z_j \operatorname{erfc}(r_{ij}/\beta_{ij}) , \quad (2.4)$$

to account for both screening effects and the lack of complete charge transfer between silicon and oxygen atoms. Such a short range potential (~ 5.5 Å) is suitable for modeling the important features of the vitreous state, but is not expected to work well for the various SiO_2 crystal structures where long range interactions play an important role.

In recent years, effective potentials involving more than just two-body interaction terms have been developed, especially in the modeling of covalently bonded systems, where the potential is expected to exhibit some directional dependence.[16–18] One such potential for silicon, due to Stillinger and Weber (SW),[16] has received much attention in MD simulations of various silicon systems. Even though the potential's parameters were determined empirically from crystalline and liquid experimental data, this short range three-body potential has been successfully applied to investigations of amorphous silicon,[19,20] silicon surfaces,[21] epitaxial growth,[22,23] and microclusters.[24,25] The SW three-body contribution is designed to lower the total binding energy when the angle formed by a central atom and two of its covalently bonded neighbors differs from the perfect tetrahedral angle, thus ensuring the potential energy minimum is ob-

tained for the optimum bonding configuration (diamond). Since the local structure of Si in silica, $Si(O_4)_{1/2}$, is also known to be tetrahedral, a three-body interaction term similar in functional form to the SW three-body term has been adopted,

$$v_3(\mathbf{r}_i,\mathbf{r}_j,\mathbf{r}_k) = h(r_{ij},r_{ik},\theta_{jik}) + h(r_{jk},r_{ji},\theta_{kji}) + h(r_{ki},r_{kj},\theta_{ikj}) \tag{2.5}$$

with

$$h(r_{ij},r_{ik},\theta_{jik}) = \begin{cases} \lambda_i \exp[\gamma_i/(r_{ij}-r_i^c) + \gamma_i/(r_{ik}-r_i^c)](\cos\theta_{jik} - \cos\theta_{jik}^c)^2, & r_{ij} < r_i^c \text{ and } r_{ik} < r_i^c \\ 0, & r_{ij} \geqslant r_i^c \text{ or } r_{ik} \geqslant r_i^c \end{cases}, \tag{2.6}$$

where λ_i, γ_i, r_i^c, and θ_{jik}^c are constants and θ_{jik} is the angle subtended by $\mathbf{r}_{ij}$ and $\mathbf{r}_{ik}$ with the vertex at i. The function $h(r_{ij},r_{ik},\theta_{jik})$ determines the three-body contribution that comes from the three atoms i, j, and k, with i as the central atom and j and k as two of its covalently bonded neighbors. Equation (2.4) is written with $\gamma_{Si} \neq \gamma_O$ and $r_{Si}^c \neq r_O^c$ to allow for differences in the local order of the two bonding configurations under consideration, O–Si–O and Si–O–Si. The three-body potential decreases the total binding energy of the system whenever the bond angle θ_{jik} differs from the preferred angle θ_{jik}^c. To impose tetrahedral geometry about Si atoms, $\theta_{O\text{-}Si\text{-}O}^c$ is set equal to the perfect tetrahedral angle, 109.471° ($\cos\theta_{O\text{-}Si\text{-}O}^c = -1/3$). Due to the presence of two lone electron pairs, oxygen also exhibits a tendency toward tetrahedral coordination as seen in the structure of ice (H_2O). Hence, $\theta_{Si\text{-}O\text{-}Si}^c$ is also set to 109.471° with the differences in the three-body interactions of the O–Si–O and Si–O–Si bonding configurations attributed to the values of λ_{Si}, λ_O, γ_{Si}, γ_O, r_{Si}^c, and r_O^c. With the tendency toward tetrahedral coordination expected to be much lower for oxygen than silicon in v-SiO_2, λ_O is anticipated to be much less than λ_{Si} and the parameter search was restricted accordingly. The distances r_{Si}^c and r_O^c denote the three-body potential cutoff for the O–Si–O and Si–O–Si configurations, respectively. Since the objective is to increase the local order about the silicon atoms and decrease the Si–O–Si bond angle in the simulated glass (with respect to the results obtained from the BMH pair potential), the cutoffs should be shorter than the appropriate second nearest neighbor distance. Results of neutron scattering and x-ray diffraction on v-SiO_2 have determined the O–O and Si–Si distances to be about 2.64 and 3.12 Å, respectively.[12,13] Therefore, after testing several values, r_{Si}^c is set to 3.0 Å and r_O^c set to 2.6 Å with the remaining three-body potential's parameters λ_{Si}, λ_O, γ_{Si}, and γ_O to be determined empirically. Unfortunately, the introduction of even a small three-body interaction term required some adjustments in the BMH pair potential's parameters, which were subsequently included in the parameter search.

III. PARAMETER SEARCH THROUGH MD SIMULATION

Despite the numerous experimental[12,13,26–28] and theoretical[29–32] studies of the vitreous SiO_2 state, its structure is still not well understood. Both continuous random network[29] (crn) and microcrystalline[30] models have been proposed to explain the structure ascertained from scattering experiments. Without a definitive structural model for total energy minimization as one would normally do for a crystal, the parameters were determined by relying upon the comparison between experiment and a glass structure obtained through MD simulations. This required a complete melt-quench sequence for each set of parameters considered. Several possible sets of parameters were first found through simulations involving 192 and 216 atoms, corresponding to MD cells started from crystalline structures of β-cristobalite and α-cristobalite, respectively. As the number of parameter sets were reduced, systems with increasing number of atoms (384, 424, and 648) were used to allow for greater relaxation. Each simulation was performed within the microcanonical ensemble with periodic boundary conditions and the volume of the MD cell scaled to correspond to the actual glass density at the simulation temperature. A time step of 0.001 ps was used with the fifth order Gear's algorithm for integrating Newton's $3N$ equations of motion.

In the melt-quench procedure, an initial configuration (either a crystalline structure or a glass structure obtained from a previous simulation) was melted at 6000 K by periodic velocity scaling during the first 3000 MD time steps. Each scaling was restricted so that the velocities did not increase more than 10% upon heating or decrease more than 3% upon cooling. Following the velocity scaling a 7 ps run at constant energy was performed to allow the system to reach internal equilibrium and to ensure memory loss of the initial configuration. The systems were then stepwise cooled to 300 K, achieving internal equilibrium at intermediate temperatures of 4000, 2000, and 1000 K. At 1000 K, the system was allowed to run at constant energy for 17 ps to encourage further structural relaxation before the final quench to 300 K. After reaching equilibrium at 300 K, the RDF, angle distributions, and bond defects were determined for each of the over 300 glasses investigated and compared to the experimental results. Since the average properties of each glass obtained by this method may vary slightly, due to the small number of atoms, several independent v-SiO_2 systems had to be generated with the same set of parameters. Composite results for the RDF and angle distributions were then calculated by averaging over these systems, before the final set of parameters were determined.

Although the three-body potential energy term has considerable effect on the glass structure formed by the melt-quench technique, the three-body contribution to the total energy is less than 0.1% of the two-body energy at 300 K. The values of the two- and three-body potential parameters which best reproduce the observed v-SiO_2 structure are given in Tables I and II. Changes in these parameters by a few percent will induce slight differences in the equilibrium in-

TABLE I. Values of the modified BMH pair potential's parameters as used in MD simulations of v-SiO_2 by Soules (Ref. 2), Garofalini (Ref. 10), and in the present simulation with three-body interactions.

	A_{Si-O}	A_{O-O} ($\times 10^{-9}$ ergs)	A_{Si-Si}	β_{Si-O}	β_{O-O} (Å)	β_{Si-Si}
Soules[b]	2.96	0.72	1.88	0.175*L~2.50[a]		
Two-body[c]	2.96	0.72	1.88	2.60	2.55	2.53
Three-body	3.00	1.10	1.88	2.29	2.34	2.34

[a] For the 192-atom systems used by Soules.
[b] Reference 2.
[c] Reference 10.

teraction distances, bond angle distributions, and the nature of the bond defects presented here, yet the conclusions summarized in Sec. V will remain qualitatively unchanged. A detailed description of the effect of the various parameters on the glass structure would be instructive but is beyond the scope of the present report and will be deferred to a subsequent publication.

IV. STRUCTURE OF THE SIMULATED GLASS

Composite results are presented for three v-SiO_2 systems, formed independently, each containing 648 atoms obtained through the MD melt-quench technique described above. The quench rate for these systems was chosen to be $\sim 10^{13}$ K/s, an order of magnitude lower than the rate used in the parameter search, allowing more sampling of the $3N$-dimensional configuration space, thus enabling the systems better access to low energy configurations. The glass at room temperature was analyzed in terms of two-body (radial distribution function) and three-body (angle distributions) correlations, number and type of bond defects, and distribution of ring sizes. A radius of 2.0 Å was used as a cutoff for defining the nearest neighbor shell about each atom with the number of bonds corresponding to the number of atoms within this shell. The coordination numbers reported here are not sensitive to slight changes in this cutoff distance since virtually all Si–O first neighbor bonds were found to be less than 1.90 Å and all O–O and Si–Si interaction distances were greater than 2.2 Å (see Fig. 1).

In addition to comparing our results with experimental data when available, they will be discussed in relation to previous MD simulation results obtained in collaboration with one of the authors (S.H.G.) using the BMH two-body potential alone.[33] The prior simulation involved a glass of 3000 atoms formed through the standard melt-quench procedure with a quench rate $\sim 10^{14}$ K/s. The radial distribution function (RDF) for the glasses obtained with the three- (solid curve) and two-body (dashed curve) potentials are presented in Fig. 1 with the results of x-ray diffraction[12(a)] and neutron scattering[13(a)] shown in Fig. 2. The first three peaks in the RDFs correspond to Si–O, O–O, and Si–Si distances, respectively. An increase in the local order about silicon atoms for the three-body glass can be readily seen by the presence of both sharp Si–O and O–O distance distributions. In the RDFs obtained from both the neutron scattering results [Fig. 2(b)] and the three-body potential, the O–O peak is found to be larger and narrower than the Si–Si peak. This is consistent with a model where the SiO_2 tetrahedral units remain intact with large variances in both the dihedral and Si–O–Si bond angles between corner sharing tetrahedra (resulting in a broad distribution of Si–Si distances) responsible for the loss of long range order. The equilibrium interaction distances were also found to be in better accord with experiment. Compared to the previous simulations, the new potential gives a slight decrease in the Si–Si interacting distance while maintaining nearly the same Si–O and O–O distances as shown in Table III. The peak and average (in parentheses) distances are given in Table III for the present simulation.

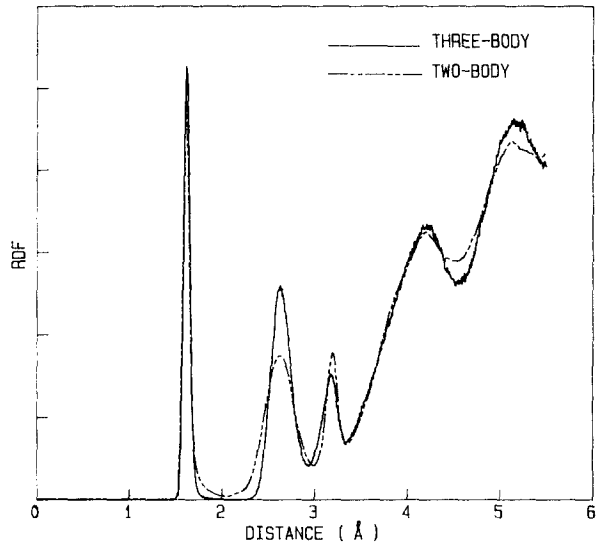

FIG 1. Radial distribution functions for v-SiO_2 obtained for a 648-atom system using the new three-body potential (solid curve) and for a 3000-atom system using a modified BMH two-body potential (dashed line).

To facilitate comparison with neutron scattering results, the static structure factor $S(q)$ is presented in Fig. 3. From Fig. 3 one sees that the $S(q)$ obtained from the simulated glass using the three-body potential (solid line) is also in good agreement with the experimental data.

The O–Si–O and Si–O–Si bond angle distributions, depicted in Fig. 4, provide further support for a glass network constructed from corner-sharing tetrahedra. One sees from Fig. 4(a) that the O–Si–O angles of the three-body glass (solid line) are narrowly distributed about the tetrahedral angle with a half-width of less than 7°. A recent calculation

TABLE II. Values used in the present simulation for the parameters of the three-body potential given in Eq. (2.6).

λ_{Si}	=	18.0×10^{-11} ergs	λ_O	=	0.3×10^{-11} ergs
γ_{Si}	=	2.6 Å	γ_O	=	2.0 Å
r^c_{Si}	=	3.0 Å	r^c_O	=	2.6 Å
$\cos\theta^c_{O-Si-O}$	=	$-1/3$	$\cos\theta^c_{Si-O-Si}$	=	$-1/3$

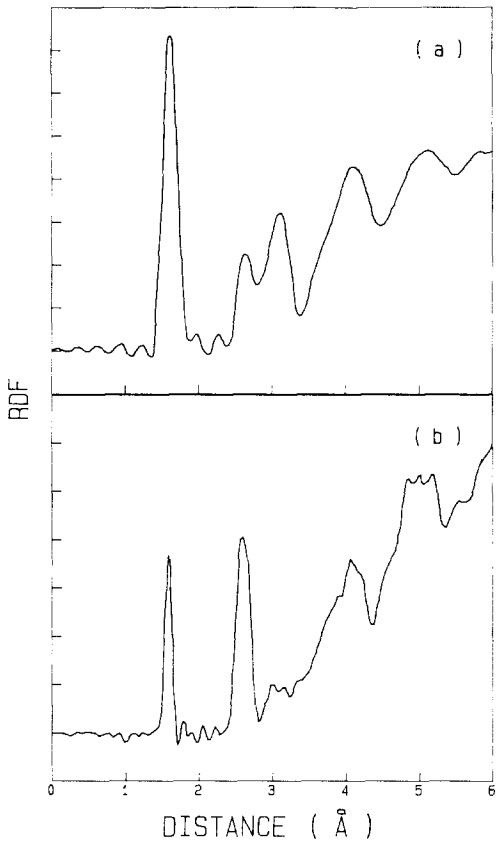

FIG. 2. Radial distribution functions obtained experimentally by (a) x-ray diffraction [Ref. 12(a)] and (b) neutron scattering [Ref. 13(a)].

based upon electron spin resonance (ESR) data also found the half-width of the O–Si–O angle distribution to be about 7°.[34] The angles between corner sharing tetrahedra [Si–O–Si angles, Fig 4(b)], determined from scattering experiments, are expected to lie between 120° and 180°, peaking between 144° and 156°. The three-body potential gives a broad distribution of Si–O–Si angles with a nearly flat peak lying between 153°–162° and an average angle of ~154°, in accord with the experimental results.

TABLE III. Comparison of equilibrium interaction distances obtained through previous MD simulations, the present MD simulation using the three-body potential and experiments. The peak position in the distance distributions is reported for the present simulations with the average interaction distances given in parentheses.

	r_{Si-O} (Å)	r_{O-O} (Å)	r_{Si-Si} (Å)
Soules[a]	1.61	2.55	3.18
Two-body[b]	1.62	2.63	3.20
Three-body	1.61 (1.62)	2.63 (2.64)	3.17 (3.14)
Expt.[c]	1.60–1.62	2.62–2.65	3.11–3.13

[a] Reference 2.
[b] Reference 33.
[c] Reference 12 and 13.

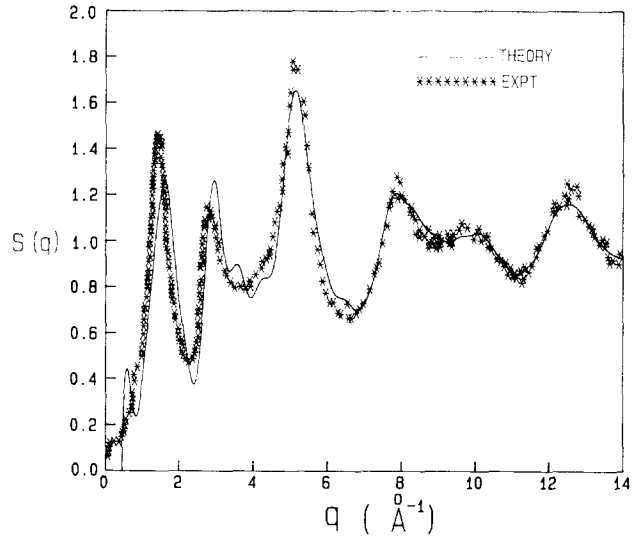

FIG. 3. The structure factor $S(q)$ found from the present simulation (solid curve) and from neutron scattering [Ref. 13(a)].

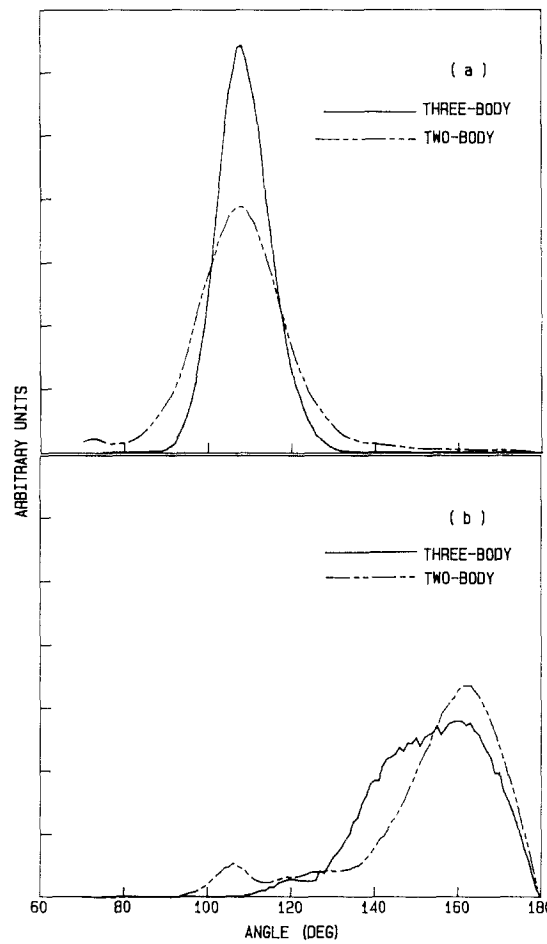

FIG. 4. (a) The O–Si–O angle distributions in v-SiO_2 formed with the three-body potential (solid curve) and the modified BMH pair potential (dashed curve). (b) The Si–O–Si angle distributions in v-SiO_2 formed with the three-body potential (solid curve) and the modified BMH pair potential (dashed curve).

Unlike glasses formed using the three-body potential, the two-body potential generates glasses which have a relatively broad distribution of O–Si–O angles and a relatively narrow distribution of Si–O–Si angles peaked at 162° [dashed curves in Figs. 4(a) and 4(b)]. In addition, such glasses contain a large number of bond defects, ~6%–8%, usually overcoordinated species, three-coordinated oxygen and five-coordinated silicon. This lack of SRO is even more pronounced in simulations of lithium and sodium silicate glasses utilizing the BMH pair potential,[2] where the average coordination of the silicon atom is unacceptably high at 4.4. Model glasses obtained with the three-body potential have much fewer bond defects (1%–2%) and are of a different nature. In the present simulations, 99.5% of the silicon were bonded to exactly four oxygen while some bond defects were manifested in three-coordinated oxygens and others in nonbridging oxygens (NBOs); silicon bond defects usually involved overcoordination, though three-coordinated Si were also identified. It is clear from the RDF and angle distributions that the three-body potential has increased the local order around the silicon atoms, i.e., well defined tetrahedral units, while broadening the distribution of angles between corner-sharing tetrahedra and lowering the concentration of bond defects with respect to the two-body potential.

The distribution of ring sizes was calculated in order to understand the effect of the three-body potential on the intermediate range order (structures of characteristic size between two and three bond lengths).[35] A ring of size N contains N-silicon atoms (or N tetrahedra), where silicon neighbors in the ring are connected through a bridging oxygen (BO). In most crystalline forms of SiO_2, all rings contain six silicon atoms. In Fig. 5, a histogram of the ring sizes for both the 3000-atom glass formed with the two-body potential (crossed) and the 648-atom glass formed with the three-body potential (striped) are presented. One can see that the average ring size of the three-body glass is higher, indicating somewhat longer range order. Still, in the present simulations, similar to the two-body results, the glass is dominated by small ring sizes with > 50% of the rings containing five Si atoms or fewer. Due to periodic boundary conditions and the relatively small number of atoms, larger rings may be restricted from forming in the present system. A relationship between the distribution of ring sizes and the quench rate was noted with a slower quench rate producing a larger average ring size. Since the results of the present simulation indicate a tendency toward larger ring sizes for the three-body potential, a MD simulation of a much larger system with a slower quench rate, which could accommodate larger rings, is presently under consideration to allow for a more accurate determination of the ring statistics.

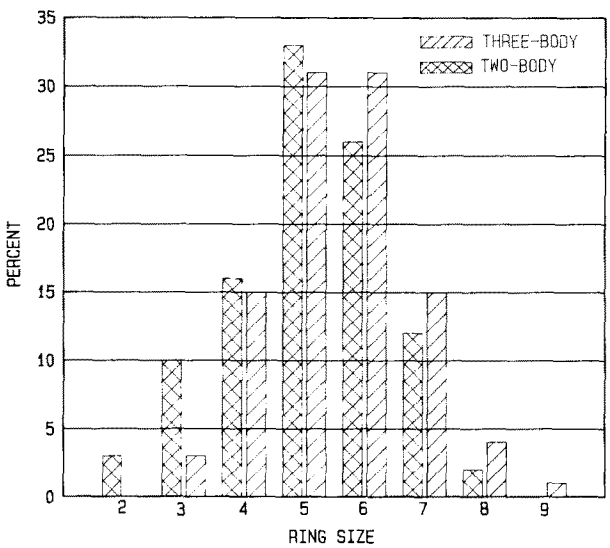

FIG. 5. Ring statistics of SiO_2 glasses formed with the three- (striped) and two-body potential (crossed).

Two-member rings, formed by edge-sharing tetrahedra, are not expected to appear in bulk silica, yet are found in the two-body glass presumably due to the lack of any directional dependence in the effective potential. Edge sharing requires large deviations in bond angles, which in the bulk is energetically unfavorable with the three-body potential, and has not been found to occur. However, three-member rings may be formed in the laboratory glass with Si–O–Si bond angles of about 130° while maintaining the O–Si–O tetrahedral angle. This strained configuration is the smallest ring size to appear in the three-body glass, yet lower in concentration than the two-body results. Since rings containing four silicon atoms may be formed in the bulk with little strain, they appear in relatively large numbers in all MD simulations of v-SiO_2 including the present one, but are only expected to appear in small numbers in the real glass.

V. SUMMARY

An empirical three-body potential for vitreous silica, suitable for computer simulations, has been constructed to reproduce similar structure as that determined from x-ray diffraction and neutron scattering experiments. The O–Si–O angle distribution is found to peak sharply about the tetrahedral angle while the Si–O–Si angles are broadly distributed between 115° and 180°, with an average of 154° in agreement with the experimental predictions. The RDF and structure factor $S(q)$ were also found to be in accord with the diffraction and scattering results. The number of bond defects are sharply reduced from previous MD simulations using pair potentials. These defects are predominantly limited to NBOs and overcoordinated oxygens with the silicon tetrahedrally bonded to exactly four oxygen. The simulated glass fits a model characterized as corner-sharing tetrahedra forming a continuous random network. But, since the microcrystalline theory of glasses estimates the glass network to be constructed of crystal-like structures of the order of 20 Å in size, the present simulation (with a box length of 21.4 Å) cannot address this possibility. Simulations of larger systems are presently underway to exploit the extra degrees of freedom for relaxation, allowing the formation of larger size rings, and the possibility of microcrystalline structures.

ACKNOWLEDGMENTS

One of the authors (B.P.F.) would like to thank Dr. R. K. Kalia for some very helpful discussions. Work supported by the Army Research Office, Grant No. DAAL03-86-K-

0047, the Center for Ceramics Research, Rutgers University, and the Fiber Optic Materials Research Program, Rutgers University. The authors would also like to acknowledge a grant of computer time on the Cyber-205 at the John von Neumann Supercomputer Center, Princeton, NJ.

[1]L. V. Woodcock, C. A. Angell, and P. Cheeseman, J. Chem. Phys. **65**, 1565 (1976).
[2]T. F. Soules, J. Chem. Phys. **71**, 4570 (1979).
[3]S. K. Mitra, M. Amini, D. Fincham, and R. W. Hockney, Philos. Mag. B **43**, 365 (1981).
[4]S. H. Garofalini, J. Chem. Phys. **76**, 3189 (1982).
[5]T. F. Soules, J. Non-Cryst. Solids **49**, 29 (1982).
[6]S. K. Mitra, Philos, Mag. B **45**, 529 (1982).
[7]S. H. Garofalini, J. Chem. Phys. **78**, 2069 (1983).
[8]S. H. Garofalini and S. Conover, J. Non-Cryst. Solids **74**, 171 (1985).
[9]S. H. Garofalini and S. M. Levine, J. Am. Ceram. Soc. **68**, 376 (1985).
[10]S. H. Garofalini and H. Melman, *Better Ceramics Through Chemistry II, MRS Symposium Proceedings*, edited by C. J. Brinker, D. E. Clark, and D. R. Ulrich (Materials Research Society, Pittsburgh, PA, 1986), Vol. 73, p. 497.
[11]A. R. Rosenthal and S. H. Garofalini, J. Am. Ceram. Soc. **70**, 821 (1987).
[12](a) R. L. Mozzi and B. E. Warren, J. Appl. Crystallogr. **2**, 164 (1969); (b) A. H. Narten, J. Chem. Phys. **56**, 1905 (1972).
[13](a) M. Misawa, D. L. Price, and K. Suzuki, J. Non-Cryst. Solids **37**, 85 (1980); (b) R. N. Sinclair and A. C. Wright, Nucl. Instrum. Methods **114**, 451 (1974).
[14]M. J. L. Sangster and M. Dixon, Adv. Phys. **25**, 247 (1976).
[15]A. Rahman, Phys. Rev. A **136**, 405 (1964).
[16]F. H. Stillinger and T. A. Weber, Phys. Rev. B **31**, 5262 (1985).
[17]R. Biswas and D. R. Hamann, Phys. Rev. Lett. **55**, 2001 (1985).
[18]J. Tersoff, Phys. Rev. Lett. **56**, 632 (1986).
[19]M. D. Kluge and J. R. Ray, Phys. Rev. B **36**, 4234 (1987).
[20]W. D. Luedtke and U. Landman, Phys. Rev. B **37**, 4656 (1988).
[21]F. F. Abraham and J. Q. Broughton, Phys. Rev. Lett. **56**, 734 (1986).
[22]M. Schneider, I. Schuller, and A. Rahman, Phys. Rev. B **36**, 1340 (1987).
[23]U. Landman, W. D. Luedtke, M. W. Ribarsky, R. N. Barnett, and C. L. Cleveland, Phys. Rev. B **37**, 4647 (1988).
[24]E. Blaisten-Barojas and D. Leveque, Phys. Rev. B **34**, 3910 (1986).
[25]B. P. Feuston, R. K. Kalia, and P. Vashishta, Phys. Rev. B **35**, 6222 (1987).
[26]A. J. Leadbetter and M. W. Stringfellow, *Neutron Inelastic Scattering* (International Atomic Energy Agency, Vienna, 1974), p. 501.
[27]M. Haas, J. Phys. Chem. Solids **31**, 415 (1970).
[28]F. L. Galeener, A. J. Leadbetter, and M. W. Stringfellow, Phys. Rev. B **27**, 1052 (1983).
[29]R. J. Bell and P. Dean, Nature **212**, 1354 (1966).
[30]K. S. Evstropyev and E. A. Porai-Koshits, J. Non-Cryst. Solids **11**, 170 (1970).
[31]P. N. Sen and M. F. Thorpe, Phys. Rev. B **15**, 4030 (1977).
[32]S. W. de Leeuw, H. He, and M. F. Thorpe, Solid State Commun. **56**, 343 (1985).
[33]D. M. Zirl and S. H. Garofalini (unpublished).
[34]A. Edwards, Army Signal Corp. (private communication).
[35]F. L. Galeener, Solid State Commun. **44**, 1037 (1982).